

CrossMark  
click for updatesCite this: *Chem. Sci.*, 2015, 6, 5690

# Carbon nitride–TiO<sub>2</sub> hybrid modified with hydrogenase for visible light driven hydrogen production†

Christine A. Caputo,<sup>a</sup> Lidong Wang,<sup>b</sup> Radim Beranek<sup>b</sup> and Erwin Reisner<sup>\*a</sup>

A system consisting of a [NiFeSe]–hydrogenase (H<sub>2</sub>ase) grafted on the surface of a TiO<sub>2</sub> nanoparticle modified with polyheptazine carbon nitride polymer, melon (CN<sub>x</sub>) is reported. This semi-biological assembly shows a turnover number (TON) of more than  $5.8 \times 10^5$  mol H<sub>2</sub> (mol H<sub>2</sub>ase)<sup>−1</sup> after 72 h in a sacrificial electron donor solution at pH 6 during solar AM 1.5 G irradiation. An external quantum efficiency up to 4.8% for photon-to-hydrogen conversion was achieved under irradiation with monochromatic light. The CN<sub>x</sub>–TiO<sub>2</sub>–H<sub>2</sub>ase construct was also active under UV-free solar light irradiation ( $\lambda > 420$  nm), where it showed a substantially higher activity than TiO<sub>2</sub>–H<sub>2</sub>ase and CN<sub>x</sub>–H<sub>2</sub>ase due, in part, to the formation of a CN<sub>x</sub>–TiO<sub>2</sub> charge transfer complex and highly productive electron transfer to the H<sub>2</sub>ase. The CN<sub>x</sub>–TiO<sub>2</sub>–H<sub>2</sub>ase system sets a new benchmark for photocatalytic H<sub>2</sub> production with a H<sub>2</sub>ase immobilised on a noble- and toxic-metal free light absorber in terms of visible light utilisation and stability.

Received 5th June 2015  
Accepted 29th June 2015

DOI: 10.1039/c5sc02017d

www.rsc.org/chemicalscience

## Introduction

The use of efficient electrocatalysts in artificial photocatalytic schemes has been an area of recent interest for the conversion of protons to hydrogen using sunlight. Specifically, the use of redox enzymes in photocatalytic schemes highlights the importance of investigating the compatibility of biological systems with light harvesting materials and testing the stability of the resultant bio-hybrid assemblies.<sup>1</sup> Hydrogenases (H<sub>2</sub>ases) are the most efficient noble-metal free electrocatalysts for H<sub>2</sub> production and achieve a turnover frequency (TOF) of more than 1000 s<sup>−1</sup> with a small overpotential.<sup>2</sup> H<sub>2</sub>ases also show impressive H<sub>2</sub> production rates and yields in sacrificial photocatalytic schemes in pH neutral aqueous solution.<sup>1a</sup> In these systems, a photoexcited light absorber provides electrons to the protein *via* an internal wire, the iron–sulfur electron relay, to the active site where proton reduction occurs. Examples are the immobilization of a H<sub>2</sub>ase on Ru-sensitised TiO<sub>2</sub>,<sup>3</sup> on Cd-based quantum dots<sup>4</sup> as well as homogeneous systems using the H<sub>2</sub>ase with a covalently linked photosystem I<sup>5</sup> or in combination with an organic dye,<sup>6</sup> and multi-component systems with a dye and a soluble redox mediator.<sup>7</sup>

Polymeric carbon nitride (polyheptazine or melon, herein CN<sub>x</sub>) is a promising visible-light absorber for the photocatalytic generation of H<sub>2</sub>.<sup>8</sup> We have recently reported the use of CN<sub>x</sub> as a light harvesting material in combination with a H<sub>2</sub>ase and a H<sub>2</sub>ase-inspired synthetic Ni catalyst for solar H<sub>2</sub> generation.<sup>9</sup> The CN<sub>x</sub>–H<sub>2</sub>ase system showed sustained catalysis with a turnover number (TON) of more than 50 000 after 70 h solar light irradiation. However, this hybrid system suffered from a weak interaction between the H<sub>2</sub>ase and the CN<sub>x</sub> surface, and consequently, poor electron transfer from CN<sub>x</sub> to the H<sub>2</sub>ase. Furthermore, CN<sub>x</sub>–H<sub>2</sub>ase only showed efficient H<sub>2</sub> production up to wavelengths of approximately 420 nm and therefore only limited visible light harvesting capabilities.

Here, we selected a hybrid material consisting of TiO<sub>2</sub> (Hombikat UV 100, anatase, BET surface area: 300 m<sup>2</sup> g<sup>−1</sup>, crystallite size < 10 nm) surface-modified with CN<sub>x</sub> polymer as a light absorbing hybrid material for the photocatalytic system with a H<sub>2</sub>ase for three main reasons (Fig. 1; see ESI and Fig. S1† for synthesis and characterisation). Firstly, CN<sub>x</sub>–TiO<sub>2</sub> can be readily prepared on a gram scale by heating TiO<sub>2</sub> nanoparticles in the presence of urea, an inexpensive and sustainable material.<sup>10</sup>

Secondly, CN<sub>x</sub>–TiO<sub>2</sub> provides us with substantially improved solar light harvesting performance compared to individual CN<sub>x</sub> and TiO<sub>2</sub>. *Band gap excitation* of TiO<sub>2</sub> (pathway 1; Fig. 1) efficiently utilises the UV spectrum (band gap of 3.2 eV for anatase TiO<sub>2</sub> with CB<sub>TiO<sub>2</sub></sub> at approximately −0.6 V vs. NHE at pH 6).<sup>11</sup> A significant portion of the visible spectrum is utilised with CN<sub>x</sub>–TiO<sub>2</sub> as it can, upon photo-excitation of CN<sub>x</sub>, perform *photoinduced electron transfer* from the LUMO<sub>CN<sub>x</sub></sub> to CB<sub>TiO<sub>2</sub></sub> (pathway 2).

<sup>a</sup>Christian Doppler Laboratory for Sustainable SynGas Chemistry, Department of Chemistry, Cambridge University, Lensfield Road, Cambridge CB2 1EW, UK. E-mail: reisner@ch.cam.ac.uk; Web: <http://www-reisner.ch.cam.ac.uk>

<sup>b</sup>Faculty of Chemistry and Biochemistry, Ruhr-Universität Bochum, Universitätsstraße 150, 44780 Bochum, Germany

† Electronic supplementary information (ESI) available. See DOI: 10.1039/c5sc02017d

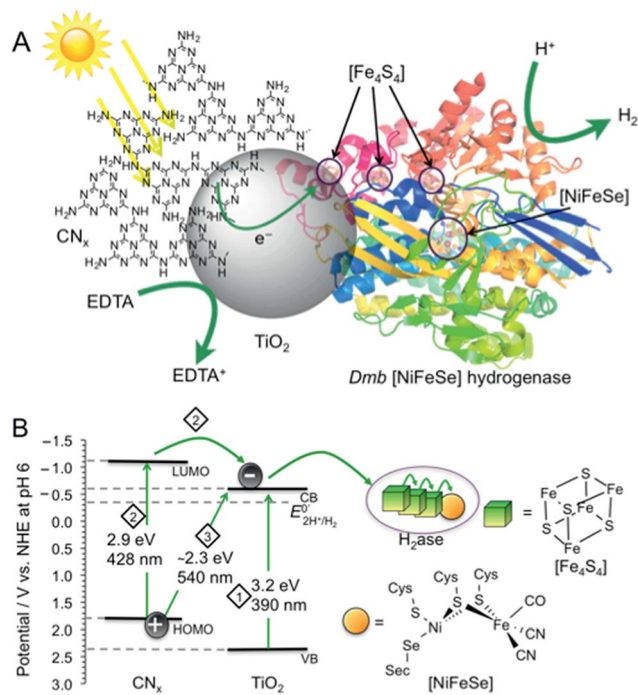


Fig. 1 (A) Schematic representation of photo- $\text{H}_2$  production with *Dmb* [NiFeSe]– $\text{H}_2$ ase (PDB ID: 1CC1)<sup>14</sup> on  $\text{CN}_x$ – $\text{TiO}_2$  suspended in water containing EDTA as a hole scavenger. (B) Irradiation of  $\text{CN}_x$ – $\text{TiO}_2$  can result in photo-induced electron transfer by three distinct pathways: (1)  $\text{TiO}_2$  band gap excitation (2) excitation of  $\text{CN}_x$  ( $\text{HOMO}_{\text{CN}_x}$ – $\text{LUMO}_{\text{CN}_x}$ ), followed by electron transfer from  $\text{LUMO}_{\text{CN}_x}$  into the conduction band of  $\text{TiO}_2$  ( $\text{CB}_{\text{TiO}_2}$ ). (3) Charge transfer excitation with direct optical electron transfer from  $\text{HOMO}_{\text{CN}_x}$  to  $\text{CB}_{\text{TiO}_2}$ . The  $\text{CB}_{\text{TiO}_2}$  electrons generated through pathways 1 to 3 are then transferred via the  $[\text{Fe}_4\text{S}_4]$  clusters to the [NiFeSe]  $\text{H}_2$ ase active site.

In addition, *direct optical electron transfer* can occur from the  $\text{HOMO}_{\text{CN}_x}$  (with contributions of molecular orbitals formed upon interaction of  $\text{CN}_x$  with  $\text{TiO}_2$ )<sup>12</sup> directly to the  $\text{CB}_{\text{TiO}_2}$  (pathway 3), extending the absorption even further into the visible region (up to 540 nm). This absorption pathway 3 is based on strong coupling between  $\text{CN}_x$  covalently grafted onto  $\text{TiO}_2$ , resulting in strong charge-transfer absorption. Conclusive evidence of this charge-transfer includes previously reported spectroscopic, photoelectrochemical, and theoretical investigations.<sup>12,13</sup> The generated  $\text{CB}_{\text{TiO}_2}$  electrons provide the  $\text{H}_2$ ase with an overpotential of approximately 0.2 V for proton reduction.

Thirdly, the  $\text{H}_2$  evolution catalyst employed in this study, *Desulfomicrobium baculatum* (*Dmb*) [NiFeSe]–hydrogenase is not only known for its high  $\text{H}_2$  evolution activity, lack of  $\text{H}_2$  inhibition and  $\text{O}_2$ -tolerance,<sup>6,14b,14c,15</sup> but also for its *titaniaphilicity*.<sup>3a</sup> This high affinity of the enzyme to adsorb strongly to  $\text{TiO}_2$  stems presumably from a protein surface rich in glutamatic and aspartic acid residues close to the distal  $[\text{Fe}_4\text{S}_4]$  cluster, which act as anchor sites to  $\text{TiO}_2$  and allow for stable binding and efficient electron flow into the hydrogenase active site (Fig. 1A).<sup>1a,3a</sup> Thus, the  $\text{CN}_x$ – $\text{TiO}_2$  hybrid is expected to support a more robust  $\text{H}_2$ ase-particle interaction than with  $\text{CN}_x$  alone,

which would result in improved charge transfer and ultimately increased catalytic turnover for  $\text{H}_2$  production.

## Results and Discussion

Photocatalytic systems were assembled by dispersing  $\text{CN}_x$ – $\text{TiO}_2$  particles in an aqueous electron donor solution (0.1 M; 2.98 mL) in a photoreactor vessel (headspace volume: 4.74 mL; see ESI† for experimental details). The vessel was sonicated under air (15 min) before sealing and purging with an inert gas (2%  $\text{CH}_4$  in  $\text{N}_2$ ). The  $\text{H}_2$ ase (16.5  $\mu\text{L}$ , 3  $\mu\text{M}$ ) was then added and the photoreactor purged again to ensure anaerobic conditions. The stirred suspension was irradiated at 25  $^\circ\text{C}$  with a solar light simulator (air mass 1.5 global filter,  $I = 100 \text{ mW cm}^{-2}$ ) and the headspace  $\text{H}_2$  was quantified at regular time intervals by gas chromatography against the internal  $\text{CH}_4$  standard. The conditions were optimised for maximum turnover frequency ( $\text{TOF}_{\text{H}_2\text{ase}}$ ) by varying the electron donor and pH of the solution (Table S1; Fig. S2 and S3†). Optimised conditions consisted of ethylenediamine tetraacetic acid (EDTA; 0.1 M) as the electron donor at pH 6. A ratio of semiconductor (5 mg unless otherwise noted) to  $\text{H}_2$ ase (50 pmol) was used for ease of comparison to previously reported photosystems with *Dmb* [NiFeSe]– $\text{H}_2$ ase.<sup>3,6,9</sup>

Solar (UV-visible) irradiation ( $\lambda > 300 \text{ nm}$ ) of  $\text{CN}_x$ – $\text{TiO}_2$ – $\text{H}_2$ ase under standard conditions generated an initial  $\text{TOF}_{\text{H}_2\text{ase}}$  of  $(2.8 \pm 0.3) \times 10^4 \text{ h}^{-1}$  or  $8 \text{ s}^{-1}$  with the production of  $5.85 \pm 0.59 \mu\text{mol H}_2$  after 4 h and  $28 \pm 3 \mu\text{mol H}_2$  with an overall  $\text{TON}_{\text{H}_2\text{ase}} > (5.8 \pm 0.6) \times 10^5$  after 72 h (Fig. 2 and S4†). Negligible amounts of  $\text{H}_2$  were detected in the absence of  $\text{H}_2$ ase,  $\text{CN}_x$ – $\text{TiO}_2$  or EDTA. UV band gap excitation of  $\text{TiO}_2$  did not result in the accumulation of  $\text{O}_2$ , which suggests that holes generated upon UV band gap excitation of  $\text{TiO}_2$  are either efficiently quenched by EDTA directly or scavenged after being trapped by  $\text{CN}_x$ .

To qualitatively determine the contributions from the three excitation pathways in Fig. 1B, irradiation was also performed with different long-pass filters. The  $\text{CN}_x$ – $\text{TiO}_2$ – $\text{H}_2$ ase system was studied under visible light irradiation at  $\lambda > 420 \text{ nm}$  to study the contribution of  $\text{CN}_x$  to light absorption (pathways 2 & 3) without

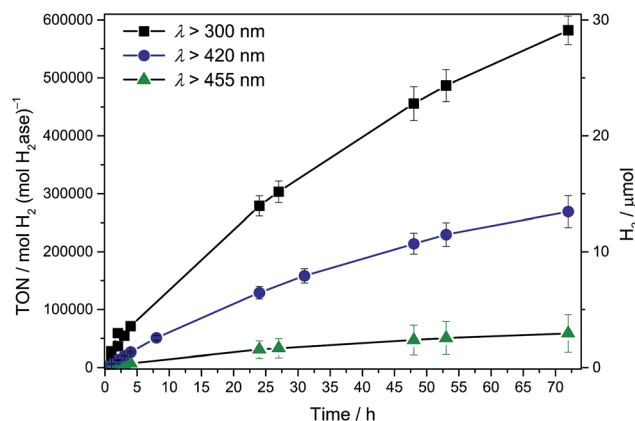


Fig. 2 Photocatalytic  $\text{H}_2$  production with *Dmb* [NiFeSe]– $\text{H}_2$ ase (50 pmol) with  $\text{CN}_x$ – $\text{TiO}_2$  (5 mg) in EDTA (pH 6, 0.1 M, 3 mL) under AM 1.5G irradiation at an intensity of 1 Sun at  $\lambda > 300$ , 420 and 455 nm.



the contribution of intrinsic absorption by  $\text{TiO}_2$  (pathway 1). A photoactivity with an initial  $\text{TOF}_{\text{H}_2\text{ase}}$  of  $6353 \pm 635 \text{ h}^{-1}$  was observed, which results in the generation of  $1.31 \pm 0.13 \mu\text{mol H}_2$  after 4 h. After 72 h,  $13 \pm 1 \mu\text{mol}$  of  $\text{H}_2$  were generated with a  $\text{TON}_{\text{H}_2\text{ase}}$  of more than  $(2.6 \pm 0.3) \times 10^5$  (Fig. 2).

Subsequently, irradiation was carried out at  $\lambda > 455 \text{ nm}$  to investigate the contribution of the direct charge-transfer from the  $\text{HOMO}_{\text{CN}_x}$  to  $\text{CB}_{\text{TiO}_2}$  to the photoactivity. A  $\text{TOF}_{\text{H}_2\text{ase}}$  of  $1096 \pm 175 \text{ h}^{-1}$  with the evolution of  $0.26 \pm 0.06 \mu\text{mol H}_2$  after 4 h and  $2.9 \pm 1.6 \mu\text{mol H}_2$  after 72 h was observed, which corresponds to 17% of the visible light activity. This suggests that all three pathways in Fig. 1B contribute to the UV-vis photoactivity, whereas pathways 2 and 3 are responsible for the visible-light response of  $\text{CN}_x\text{-TiO}_2\text{-H}_2\text{ase}$ . Previous investigations of  $\text{CN}_x\text{-TiO}_2$  hybrids have shown that their activity is limited by the strong electronic coupling between  $\text{CN}_x$  and  $\text{TiO}_2$  leading not only to intense visible light absorption but also to fast back electron transfer (primary recombination).<sup>13,16</sup>

In order to study the role of  $\text{TiO}_2$  as heterogeneous electron relay in  $\text{CN}_x\text{-TiO}_2\text{-H}_2\text{ase}$  in more detail, a sample of  $\text{CN}_x\text{-ZrO}_2$  (15 mg) was also tested with the  $\text{H}_2\text{ase}$ . The negative  $\text{CB}_{\text{ZrO}_2}$  at approximately  $-1.35 \text{ V vs. NHE}$  at pH 6, prevents electron injection from  $\text{LUMO}_{\text{CN}_x}$  (approximately  $-1.25 \text{ V vs. NHE}$  at pH 6).<sup>17</sup> This band level mismatch allowed us to demonstrate that spatial proximity of surface-bound  $\text{H}_2\text{ase}$  to  $\text{CN}_x$  alone cannot promote productive electron transfer as no  $\text{H}_2$  was observed with  $\text{CN}_x\text{-ZrO}_2\text{-H}_2\text{ase}$  ( $\lambda > 300 \text{ nm}$ ; Fig. S4†). Thus, charge transfer from the  $\text{LUMO}_{\text{CN}_x}$  into  $\text{CB}_{\text{ZrO}_2}$  (pathway 2) is not possible, nor is the direct electron transfer from  $\text{HOMO}_{\text{CN}_x}$  to  $\text{CB}_{\text{ZrO}_2}$  (pathway 3), which are crucial to the formation of  $\text{H}_2$  with the hybrid material.

For comparison,  $\text{H}_2$  production was also tested with  $\text{CN}_x$  (5 mg) and  $\text{H}_2\text{ase}$  (50 pmol) in the absence of metal oxide under standard conditions. A  $\text{TON}_{\text{H}_2\text{ase}}$  of  $14852 \pm 1485$  was obtained after 4 h with an initial TOF of  $6288 \pm 649 \text{ h}^{-1}$  when irradiated with UV-visible light ( $\lambda > 300 \text{ nm}$ , Table S1†). Under visible light irradiation ( $\lambda > 420 \text{ nm}$ ), a  $\text{TON}_{\text{H}_2\text{ase}}$  of  $2375 \pm 267$  was observed after 4 h and no  $\text{H}_2$  was produced at  $\lambda > 455 \text{ nm}$ , demonstrating the substantially enhanced activity with  $\text{CN}_x\text{-TiO}_2\text{-H}_2\text{ase}$  compared to  $\text{CN}_x\text{-H}_2\text{ase}$  at all wavelengths (Fig. S4†).

Experiments were also performed with  $\text{TiO}_2\text{-H}_2\text{ase}$ . While the system showed comparable activity under UV-visible irradiation due to efficient band gap excitation of  $\text{TiO}_2$  (pathway 1), it showed significantly reduced activity under visible only irradiation at  $\lambda > 420 \text{ nm}$  and displayed negligible  $\text{H}_2$  yields at  $\lambda > 455 \text{ nm}$  compared to  $\text{CN}_x\text{-TiO}_2\text{-H}_2\text{ase}$  (Fig. S4†).<sup>9</sup> Thus, UV-band gap excitation of  $\text{TiO}_2$  dominates the absorption of the  $\text{CN}_x\text{-TiO}_2\text{-H}_2\text{ase}$  hybrid material under UV-light irradiation, which becomes less significant under visible irradiation.

The effect of light intensity on the photocatalytic activity ( $\lambda > 300 \text{ nm}$ ) was studied by employing neutral density filters. A photoactivity of approximately 90% remained when employing a 50% absorbance filter ( $50 \text{ mW cm}^{-2}$ ) and 44% of activity remained with an 80% filter ( $20 \text{ mW cm}^{-2}$ ; Fig. S5†). The initial non-linear decrease in activity implies that the system is not limited by light at 1 Sun intensity as has been observed

previously with synthetic  $\text{H}_2$  evolution catalyst-modified Ru dye-sensitised  $\text{TiO}_2$  systems.<sup>18</sup>

The  $\text{CN}_x\text{-TiO}_2\text{-H}_2\text{ase}$  system sets a new benchmark for visible light driven and prolonged  $\text{H}_2$  production with a heterogenised  $\text{H}_2\text{ase}$  without the need for expensive or toxic materials.<sup>3,4,9</sup> A part of this improvement can be attributed to the direct optical electron transfer (pathway 3) within  $\text{CN}_x\text{-TiO}_2$ , which draws the absorption of solar light significantly into the visible spectrum.

The enzyme loading onto  $\text{CN}_x\text{-TiO}_2$  was calculated based on the BET surface area of  $111 \text{ m}^2 \text{ g}^{-1}$ , a crystallite surface area of  $\sim 314 \text{ nm}^2$  per particle and an estimation that approximately one-quarter of the surface area of  $\text{TiO}_2$  is accessible for the enzyme to adsorb. This equates to  $\sim 0.1 \text{ H}_2\text{ase}$  per particle of  $\text{CN}_x\text{-TiO}_2$ . The approximate 1 : 10 enzyme : particle ratio allows the  $\text{H}_2\text{ase}$  to function at the maximum rate (*i.e.*, TOF) as the maximum electron flux of conduction band electrons is directed towards a single enzyme. To qualitatively determine the amounts of surface-bound and solubilised  $\text{H}_2\text{ase}$  in the optimised system,  $\text{H}_2\text{ase}$  (50 pmol) was loaded onto  $\text{CN}_x\text{-TiO}_2$  (5 mg) in aqueous EDTA solution by stirring under  $\text{N}_2$  for 15 min. The suspension was centrifuged and the supernatant decanted (see ESI† for experimental details). The  $\text{CN}_x\text{-TiO}_2\text{-H}_2\text{ase}$  pellet was re-dispersed in fresh EDTA solution (3 mL, 0.1 M, pH 6) and the photocatalytic vessel purged with 2%  $\text{CH}_4$  in  $\text{N}_2$ . The suspension was then irradiated ( $\lambda > 420 \text{ nm}$ ) and  $\text{H}_2$  production monitored (Fig. 3). The  $\text{H}_2$  production activity was nearly identical to a sample that was not centrifuged, both in the presence and absence of methyl viologen ( $\text{MV}^{2+}$ , see below), indicating that attachment of  $\text{H}_2\text{ase}$  to  $\text{CN}_x\text{-TiO}_2$  is essentially quantitative. The substantially improved adsorption of the enzyme on the  $\text{TiO}_2$  surface compared to the inert  $\text{CN}_x$  polymer therefore also contributes to the increased activity of  $\text{CN}_x\text{-TiO}_2\text{-H}_2\text{ase}$  compared to  $\text{CN}_x\text{-H}_2\text{ase}$ . Previously an 88% decrease in photoactivity was observed with the poorly interacting  $\text{CN}_x\text{-}$



Fig. 3 Photocatalytic  $\text{H}_2$  production using *Dmb* [NiFeSe]- $\text{H}_2\text{ase}$  (50 pmol) in EDTA (pH 6, 0.1 M, 3 mL) with  $\text{CN}_x\text{-TiO}_2$  (5 mg) under optimised conditions before and after centrifugation and re-suspension in fresh EDTA buffer solution followed by 1 Sun irradiation ( $\lambda > 420 \text{ nm}$ ). Results are also shown in the presence and absence of redox mediator, methyl viologen ( $\text{MV}^{2+}$ ).





H<sub>2</sub>ase after centrifugation and re-dispersion in fresh electron donor buffer.<sup>9</sup>

The external quantum efficiency (EQE) of the CN<sub>x</sub>-TiO<sub>2</sub>-H<sub>2</sub>ase system was measured by applying narrow band pass filters ( $\lambda = 360 \pm 10$  nm;  $I = 2.49$  mW cm<sup>-2</sup> and  $400 \pm 10$  nm;  $I = 4.34$  mW cm<sup>-2</sup>; see ESI† for experimental details). UV-irradiation gave an EQE of approximately 4.8% and under visible irradiation an EQE of 0.51% was obtained. These values are more than a 10-fold improvement over the UV and visible EQE for the CN<sub>x</sub>-H<sub>2</sub>ase system,<sup>9</sup> which can be attributed to the improved light absorption (Fig. S6†) and increased electron transfer rate due to adsorption of the H<sub>2</sub>ase onto the particle surface.

We previously showed that a significantly increased photoactivity was observed under standard conditions using CN<sub>x</sub>-H<sub>2</sub>ase upon addition of an excess of the redox mediator MV<sup>2+</sup>, producing up to 77  $\mu$ mol H<sub>2</sub> after 69 h of UV-visible irradiation.<sup>9</sup> A long-term experiment with H<sub>2</sub>ase (50 pmol), CN<sub>x</sub>-TiO<sub>2</sub> (5 mg) and added MV<sup>2+</sup> (5  $\mu$ mol) in aqueous EDTA (0.1 M) at pH 6 was performed with both  $\lambda > 300$  nm light and with visible light only ( $\lambda > 420$  nm). Under UV-visible irradiation after 72 h, the CN<sub>x</sub>-TiO<sub>2</sub>-MV-H<sub>2</sub>ase system produced 193  $\mu$ mol H<sub>2</sub> with a TON<sub>H<sub>2</sub>ase</sub> of  $> 3.8 \times 10^6$  and an initial TOF<sub>H<sub>2</sub>ase</sub> of 35 s<sup>-1</sup> (Fig. S7†). Under visible-light only, 66  $\mu$ mol H<sub>2</sub> was produced with a TON<sub>H<sub>2</sub>ase</sub> of  $1.3 \times 10^6$  and an initial TOF<sub>H<sub>2</sub>ase</sub> of 9 s<sup>-1</sup> (Fig. S8†). The ratio of the amount of hydrogen produced in the presence and absence of MV<sup>2+</sup> can be used to estimate the relative efficiency of the charge transfer from material to H<sub>2</sub>ase. Under full spectrum irradiation ( $\lambda > 300$  nm) with CN<sub>x</sub>-H<sub>2</sub>ase the ratio was found to be 22, whereas for both TiO<sub>2</sub>-H<sub>2</sub>ase and CN<sub>x</sub>-TiO<sub>2</sub>-H<sub>2</sub>ase systems the ratio was 5. This strongly supports the fact that there is a significant improvement in the charge transfer from a TiO<sub>2</sub>-based material to H<sub>2</sub>ase. In addition, this ratio remains constant when the wavelength of light used is restricted to the visible region ( $\lambda > 420$  nm).

The H<sub>2</sub> production rates in the presence of MV<sup>2+</sup> are significantly higher than those obtained in the absence of MV<sup>2+</sup>. The blue colour of the vials containing MV<sup>2+</sup> is indicative of the formation of reduced MV<sup>•+</sup> in solution (Fig. S9†). By comparison, addition of MV<sup>2+</sup> to the previously reported Ru-dye-sensitised TiO<sub>2</sub>-H<sub>2</sub>ase system caused a slight decrease in activity, which was attributed to the decreased availability of electrons for the H<sub>2</sub>ase and the absorption of incident photons by MV<sup>•+</sup>.<sup>3a</sup> Here, solubilised MV<sup>•+</sup> does not limit light absorption by CN<sub>x</sub>-TiO<sub>2</sub> significantly and is able to efficiently donate electrons to surface-bound H<sub>2</sub>ase, resulting in increased H<sub>2</sub> production. This result implies that interfacial electron transfer from CN<sub>x</sub>-TiO<sub>2</sub> to H<sub>2</sub>ase is still not fully optimised in this system, where the orientation of the H<sub>2</sub>ase is not fully 'directed'. Ideally, the distance from the CN<sub>x</sub>-TiO<sub>2</sub> surface to the [Fe<sub>4</sub>S<sub>4</sub>] electron transport chain should be minimised and an improved orientation of the enzyme would allow trapping of CB<sub>TiO<sub>2</sub></sub> electrons more efficiently for maximised turnover.<sup>19</sup>

Favourable electron transfer kinetics at the CN<sub>x</sub>-TiO<sub>2</sub>-H<sub>2</sub>ase interface can be assumed based on previous reports. Electron transfer in the order of 10<sup>7</sup> s<sup>-1</sup> was reported from CdS nanorods to an [FeFe]-H<sub>2</sub>ase isolated from *Clostridium*

*acetobutylicum*.<sup>4c</sup> In addition, a long lived photo-excited state lifetime of  $\tau_{1/2} \sim 0.8$  s was previously reported for TiO<sub>2</sub> conduction band electrons in a photocatalytic system with Ru dye-sensitised TiO<sub>2</sub> and electron transfer to co-immobilised molecular cobaloxime catalysts occurred with  $\tau_{1/2} \sim 5$  to 50  $\mu$ s.<sup>20</sup> Based on these reports, we can assume that a reasonably long-lived TiO<sub>2</sub> conduction band electron is generated and that H<sub>2</sub>ase is capable of readily collecting these electrons.

## Conclusions

In summary, solar light driven H<sub>2</sub> production with a semi-biological system consisting of TiO<sub>2</sub> modified with polymeric CN<sub>x</sub> and immobilised H<sub>2</sub>ase has been demonstrated. We have shown that by improving the surface interaction of the enzyme with the light harvesting CN<sub>x</sub> material, specifically by adsorption of the enzyme onto the TiO<sub>2</sub> surface, H<sub>2</sub> generation is drastically improved. Another important factor is the improved visible light absorption by direct CN<sub>x</sub> excitation (pathway 2) and CN<sub>x</sub>-TiO<sub>2</sub> charge transfer (pathway 3), which enables high photoactivity. The CN<sub>x</sub>-TiO<sub>2</sub>-H<sub>2</sub>ase assembly achieved a TOF of 8 s<sup>-1</sup> and TON of  $> 5.8 \times 10^5$  after 72 h in the absence of an external soluble redox mediator, thereby setting a new benchmark for photochemical architectures based on abundant and non-toxic materials and a heterogenised H<sub>2</sub>ase. The additional use of the redox mediator MV<sup>2+</sup> allowed for the photo-generation of H<sub>2</sub> with a TOF of 35 s<sup>-1</sup> and a TON of  $> 3.8 \times 10^6$ . This work advances the use of hybrid photocatalytic schemes by integrating highly active electrocatalysts with advanced light absorbing materials such as CN<sub>x</sub>-TiO<sub>2</sub>, which is shown to be compatible with H<sub>2</sub>ases in aqueous solution.

## Acknowledgements

We acknowledge support by the Christian Doppler Research Association (Austrian Federal Ministry of Science, Research and Economy and National Foundation for Research, Technology and Development), the OMV Group and a Marie Curie fellowship to C.C. (GAN 624997624997). R.B. and L.W. acknowledge financial support by the MIWFT-NRW within the project "Anorganische Nanomaterialien für Anwendungen in der Photokatalyse". We thank Dr J. C. Fontecilla-Camps and Dr C. Cavazza (CNRS Grenoble, France) for providing us with *Dmb* [NiFeSe] hydrogenase, Ms Marielle Bauzan (CNRS Marseilles, France) for growing the bacteria, and Dr Michal Bledowski for assistance with CN<sub>x</sub>-TiO<sub>2</sub> synthesis.

## Notes and references

- (a) E. Reisner, *Eur. J. Inorg. Chem.*, 2011, 1005–1016; (b) P. W. King, *Biochim. Biophys. Acta*, 2013, **1827**, 949–957.
- (a) F. A. Armstrong, N. A. Belsey, J. A. Cracknell, G. Goldet, A. Parkin, E. Reisner, K. A. Vincent and A. F. Wait, *Chem. Soc. Rev.*, 2009, **38**, 36–51; (b) A. K. Jones, E. Sillery, S. P. J. Albracht and F. A. Armstrong, *Chem. Commun.*, 2002, 866–867; (c) W. Lubitz, H. Ogata, O. Rüdiger and E. Reijerse, *Chem. Rev.*, 2014, **114**, 4081–4148.



- 3 (a) E. Reisner, D. J. Powell, C. Cavazza, J. C. Fontecilla-Camps and F. A. Armstrong, *J. Am. Chem. Soc.*, 2009, **131**, 18457–18466; (b) E. Reisner, J. C. Fontecilla-Camps and F. A. Armstrong, *Chem. Commun.*, 2009, 550–552.
- 4 (a) B. L. Greene, C. A. Joseph, M. J. Maroney and R. B. Dyer, *J. Am. Chem. Soc.*, 2012, **134**, 11108–11111; (b) A. Bachmeier, V. C. C. Wang, T. W. Woolerton, S. Bell, J. C. Fontecilla-Camps, M. Can, S. W. Ragsdale, Y. S. Chaudhary and F. A. Armstrong, *J. Am. Chem. Soc.*, 2013, **135**, 15026–15032; (c) M. B. Wilker, K. E. Shinopoulos, K. A. Brown, D. W. Mulder, P. W. King and G. Dukovic, *J. Am. Chem. Soc.*, 2014, **136**, 4316–4324.
- 5 (a) C. E. Lubner, R. Grimme, D. A. Bryant and J. H. Golbeck, *Biochemistry*, 2010, **49**, 404–414; (b) H. Krassen, A. Schwarze, B. Friedrich, K. Ataka, O. Lenz and J. Heberle, *ACS Nano*, 2009, **3**, 4055–4061; (c) M. Ihara, H. Nishihara, K.-S. Yoon, O. Lenz, B. Friedrich, H. Nakamoto, K. Kojima, D. Honma, T. Kamachi and I. Okura, *Photochem. Photobiol.*, 2006, **82**, 676–682.
- 6 T. Sakai, D. Mersch and E. Reisner, *Angew. Chem., Int. Ed.*, 2013, **52**, 12313–12316.
- 7 (a) I. Okura, *Coord. Chem. Rev.*, 1985, **68**, 53–99; (b) O. A. Zadornyy, J. E. Lucon, R. Gerlach, N. A. Zorin, T. Douglas, T. E. Elgren and J. W. Peters, *J. Inorg. Biochem.*, 2012, **106**, 151–155.
- 8 (a) X. Wang, K. Maeda, A. Thomas, K. Takanabe, G. Xin, J. M. Carlsson, K. Domen and M. Antonietti, *Nat. Mater.*, 2009, **8**, 76–80; (b) D. J. Martin, P. J. T. Reardon, S. J. A. Moniz and J. Tang, *J. Am. Chem. Soc.*, 2014, **136**, 12568–12571; (c) M. K. Bhunia, K. Yamauchi and K. Takanabe, *Angew. Chem., Int. Ed.*, 2014, **53**, 11001–11005.
- 9 C. A. Caputo, M. A. Gross, V. W. Lau, C. Cavazza, B. V. Lotsch and E. Reisner, *Angew. Chem., Int. Ed.*, 2014, **53**, 11538–11542.
- 10 (a) R. Beranek and H. Kisch, *Photochem. Photobiol. Sci.*, 2008, **7**, 40–48; (b) D. Mitoraj and H. Kisch, *Angew. Chem., Int. Ed.*, 2008, **47**, 9975–9978.
- 11 (a) A. Fujishima and K. Honda, *Nature*, 1972, **238**, 37–38; (b) M. Grätzel, *Nature*, 2001, **414**, 338–344; (c) Y. Ma, X. Wang, Y. Jia, X. Chen, H. Han and C. Li, *Chem. Rev.*, 2014, **114**, 9987–10043.
- 12 M. Bledowski, L. Wang, A. Ramakrishnan, O. V. Khavryuchenko, V. D. Khavryuchenko, P. C. Ricci, J. Strunk, T. Cremer, C. Kolbeck and R. Beranek, *Phys. Chem. Chem. Phys.*, 2011, **13**, 21511–21519.
- 13 M. Bledowski, L. Wang, A. Ramakrishnan, A. Bétard, O. V. Khavryuchenko and R. Beranek, *ChemPhysChem*, 2012, **13**, 3018–3024.
- 14 (a) E. Garcin, X. Vernede, E. C. Hatchikian, A. Volbeda, M. Frey and J. C. Fontecilla-Camps, *Structure*, 1999, **7**, 557–566; (b) A. Parkin, G. Goldet, C. Cavazza, J. C. Fontecilla-Camps and F. A. Armstrong, *J. Am. Chem. Soc.*, 2008, **130**, 13410–13416; (c) C. S. A. Baltazar, M. C. Marques, C. M. Soares, A. M. DeLacey, I. A. C. Pereira and P. M. Matias, *Eur. J. Inorg. Chem.*, 2011, 948–962.
- 15 (a) M. C. Marques, R. Coelho, A. L. De Lacey, I. A. C. Pereira and P. M. Matias, *J. Mol. Biol.*, 2010, **396**, 893–907; (b) A. Volbeda, P. Amara, M. Iannello, A. L. De Lacey, C. Cavazza and J. C. Fontecilla-Camps, *Chem. Commun.*, 2013, **49**, 7061–7063.
- 16 (a) L. Wang, M. Bledowski, A. Ramakrishnan, D. König, A. Ludwig and R. Beranek, *J. Electrochem. Soc.*, 2012, **159**, H616–H622; (b) M. Bledowski, L. Wang, S. Neubert, D. Mitoraj and R. Beranek, *J. Phys. Chem. C*, 2014, **118**, 18951–18961.
- 17 K. Sayama and H. Arakawa, *J. Phys. Chem.*, 1993, **97**, 531–533.
- 18 F. Lakadamyali, M. Kato and E. Reisner, *Faraday Discuss.*, 2012, **155**, 191–205.
- 19 A. Bachmeier and F. Armstrong, *Curr. Opin. Chem. Biol.*, 2015, **25**, 141–151.
- 20 (a) F. Lakadamyali, A. Reynal, M. Kato, J. R. Durrant and E. Reisner, *Chem.–Eur. J.*, 2012, **18**, 15464–15475; (b) A. Reynal, J. Willkomm, N. M. Muresan, F. Lakadamyali, M. Planells, E. Reisner and J. R. Durrant, *Chem. Commun.*, 2014, **50**, 12768–12771.

